**TD-06-043**
**August 11, 2006**

# A Finite Element Simulation of the Winding, Cool down, and Energizing of the Focusing Solenoid for the CH Section of the HINS Linac.

Bob Wands

## Introduction and Summary

A 2-d axisymmetric finite element model of the DTL Section solenoid was created to simulate winding, cool down, and excitation of the solenoid.

The results show that the winding tensions of 20 N and 10 N for the main coil and bucking coil, respectively, are sufficient to keep the layers of the solenoid and the bucking coils in contact with their respective spools after cool down and energizing, except for a very small region at the inner radius downstream end of the bucking coil, where some separation is seen.

The iron design, with its through-bolted flange and small initial flange-to-barrel clearance, allows the helium tube and flange bolts to effectively preload the coils and spacers when warm, and to retain that preload after cool down. This allows the relief of coil compression to contribute to the axial stiffness seen by the bucking coil, and acts to minimize bucking coil deflections.

The Lorentz forces produce axial displacements in the bucking coil of up to 24 microns. Some of this displacement can be attributed to the gap which opens up between the bucking coil and its adjacent spacer during the cool down.

## Geometry and Material Properties

The solenoid and bucking coil specifications were taken from a note by G. Davis, et. al. "Linac DTL Section Focusing Solenoid Cold Mass Design" (March 27, 2006), and related drawings.

The material properties are shown in Table I. The properties of the main spool copper were adjusted by area-reduction to account for the presence of splines on the inner diameter where the spool and helium tube mate. Doing this simplified the modeling by allowing the use of the full spool thickness. Since this technique results in the correct stiffness, but not the correct stress, the output stresses were scaled by the full copper modulus to find the approximate true stresses.

**Table I. Material Properties**

| Material | Young's Modulus – Axial (GPa) | Young's Modulus – Azimuthal (GPa) | Young's Modulus – Radial (GPa) | Thermal Contraction 293 K – 4.2 K |
|---|---|---|---|---|
| Stainless Steel | 199 | 199 | 199 | 3.1e-3 |
| Copper | 110 | 110 | 110 | 3.3e-3 |
| Copper – Main Coil Spool | 81.8 | 45.3 | 81.8 | 3.3e-3 |
| NbTi | 100 | 100 | 100 | 3.5e-3 |

## The Finite Element Model

A 2-d axisymmetric magneto-structural model was created which is capable of following the solenoid through the assembly, cool down, and energizing load steps. Interface conditions were defined to allow components to separate and/or slide where appropriate.

The winding of the main and bucking coils was simulated during the assembly load step by adjusting the conductor thermal contraction coefficient on a per-element basis to give an approximately uniform winding tension despite the non-uniform stiffness of the spools.

During the cool down load step, the thermal contraction coefficients were again adjusted on a per-element basis to give the correct total thermal contraction down to the operating temperature of 4.3 K.

The clearance between the main coil spool and the helium tube was adjusted so that at the end of winding, the two components are just touching in the central region (away from the spool flanges.)

Fig. 1 shows the finite element model (with air elements deleted for clarity). The various components are identified. Table II details the interface behavior of the components. Most notable is that the helium tube does not interact in shear with any component except the weld ring. The coil and spacer elements react only in compression with each other, and are free to separate if necessary when differential thermal contractions or Lorentz forces are active.

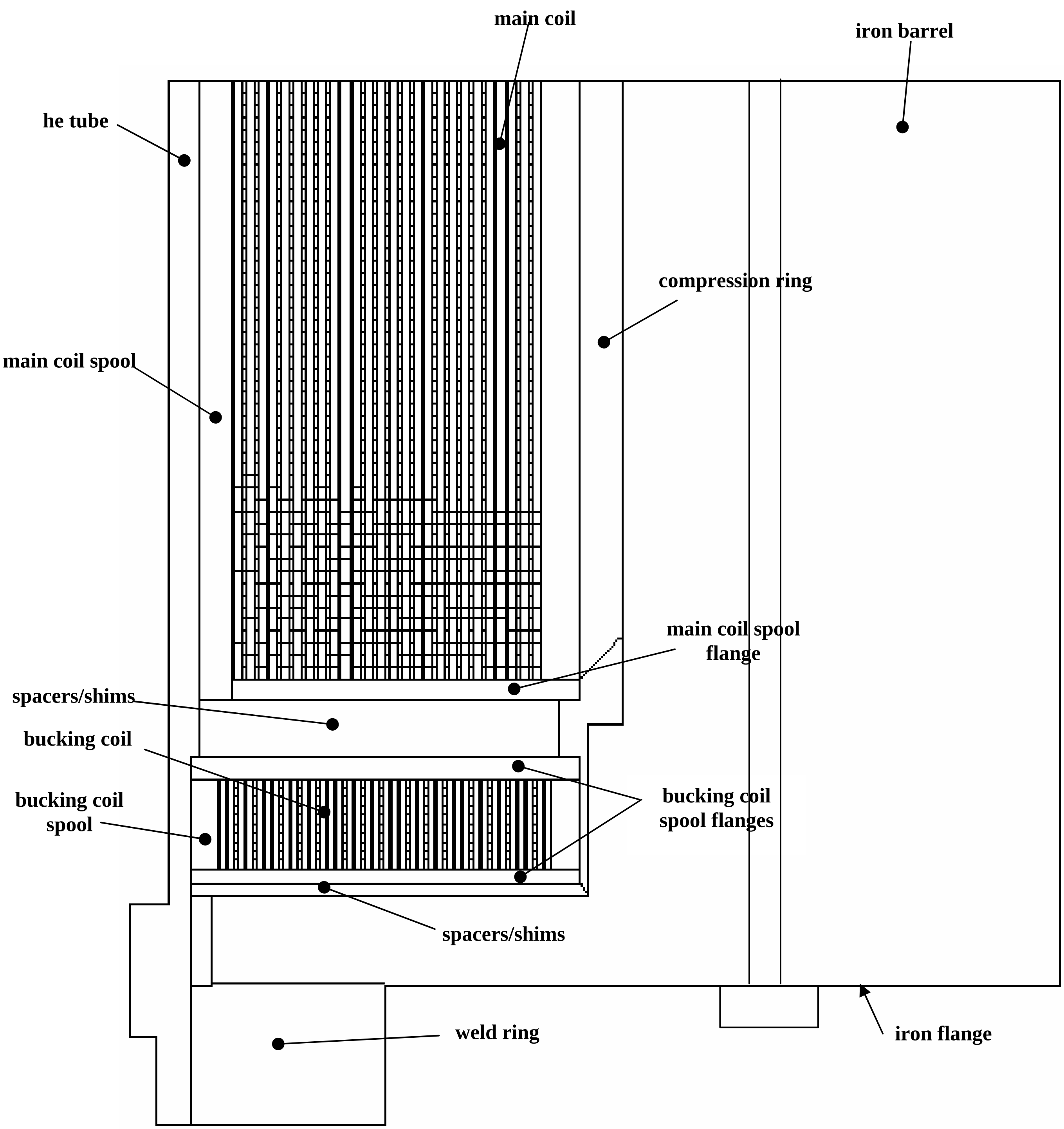


**Figure 1. Finite Element Model – Components (Air deleted for clarity)**

**Table II. Interface Characterization**

| Component 1 | Component 2 | Characterization |
|---|---|---|
| helium tube | all other | free to slide axially, and separate radially |
| main coil layer | adjacent main coil layer | free to slide axially, and separate radially |
| main coil layer | main coil spool flange | free to slide radially and separate axially |
| main coil layer 1 | main coil spool | free to slide axially and separate radially |
| bucking coil layer | adjacent bucking coil layer | free to slide axially and separate radially |
| bucking coil layer | bucking coil spool flange | free to slide radially and separate axially |
| bucking coil layer 1 | bucking coil spool | free to slide axially and separate radially |
| iron flange | aluminum spacer | free to slide radially and separate axially |
| iron flange | iron barrel | free to slide radially and separate axially – initial clearance of 0.2mm |
| spacers/shims | bucking coil and main coil spool flanges | free to slide radially and separate axially |
| spacer/shims | iron flange | free to slide radially and separate axially |

## Warm Assembly and Preload

Using gap elements with initial interferences between the tube and weld flange, and the flange bolt heads and the flange, the iron and helium tube were preloaded against the coil and spacer package until a force of approximately 13.5 kN was produced in both the helium tube and the bolts.

Fig. 2 shows the warm deflections, with preload and winding loads applied. All surfaces between the bucking coil, spacers, and iron are closed.

Fig. 3 shows the hoop stress in the main coil and bucking coil after assembly. For both the main and bucking coils, winding has produced hoop compression on the innermost layers.

Close examination of the main coil spool shows that the calculated hoop stresses are as high at 62 MPa in the central portion away from the flanges. Adjusting for the reduced material modulus, the corresponding corrected stress is 62(110/45.3) = 148 MPa. This is well above the yield stress of 90 MPa for annealed copper. This yielding will probably bring the spool into contact with the helium tube, from which it will pick up substantial stiffness.

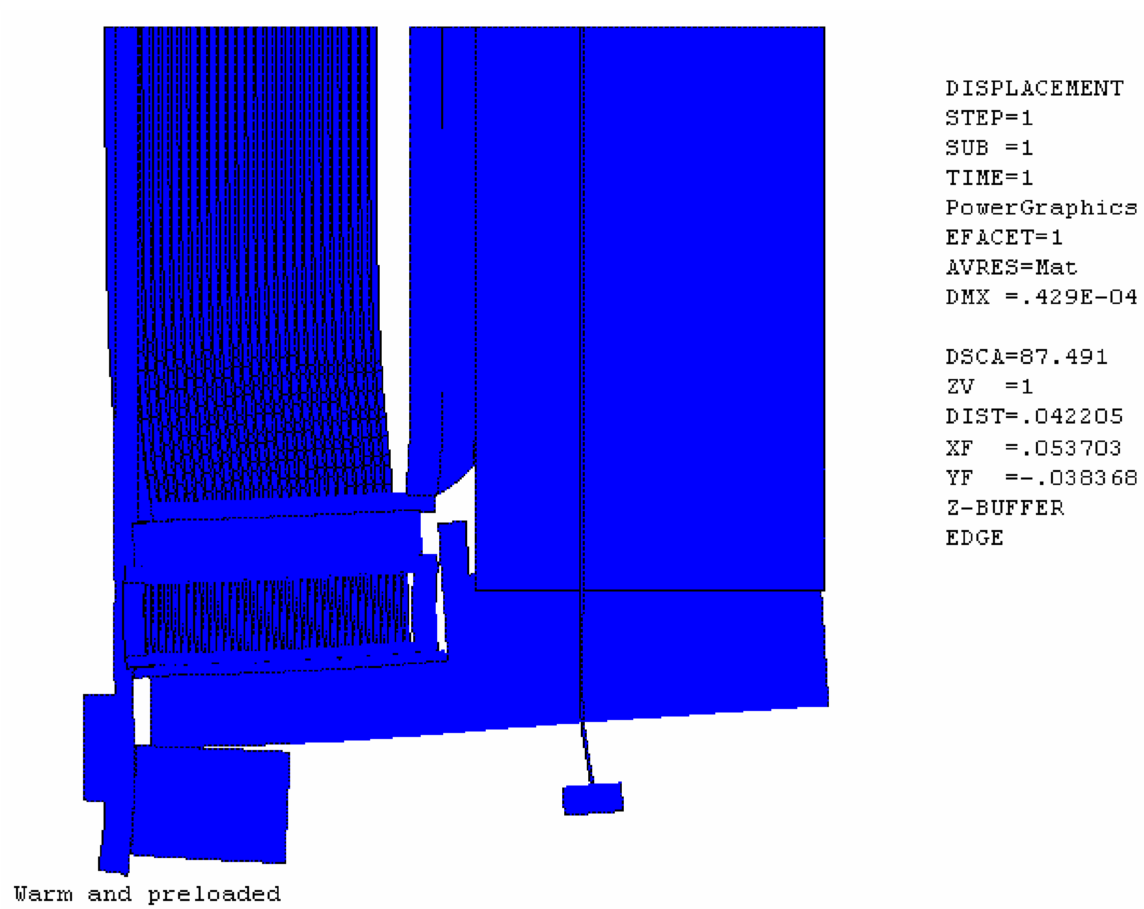


**Figure 2. Displacements – Warm and Preloaded**

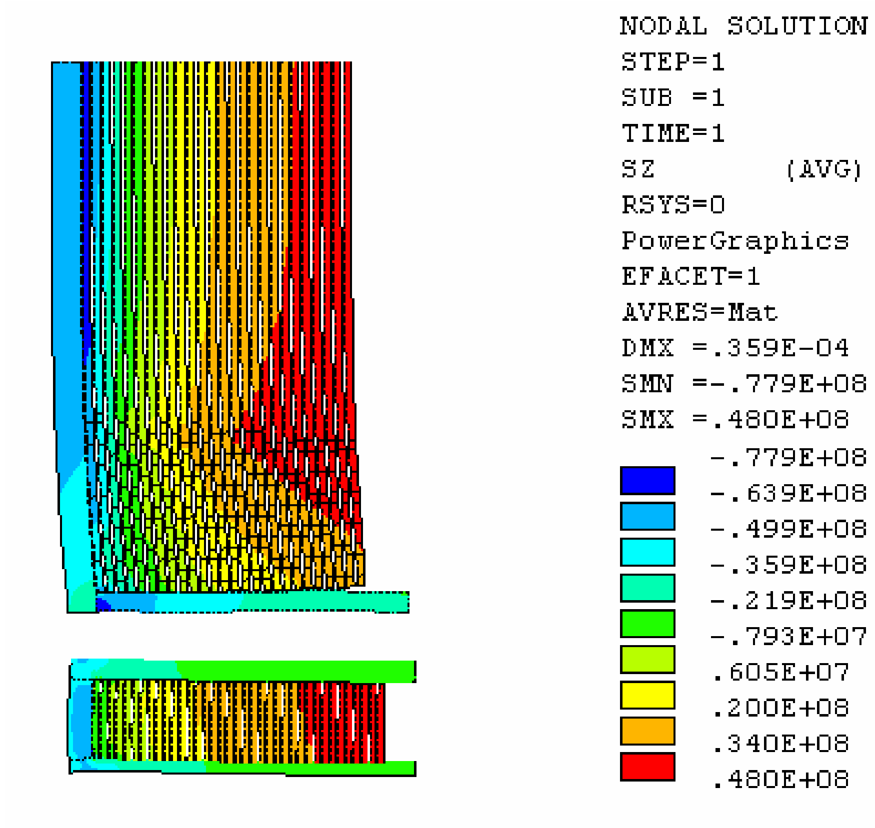


**Figure 3. HoopStresses in Main Coil and Bucking Coil after Winding and Assembly**

## Cool down

Fig. 4 shows the cold deflections. A gap of about 6 microns has opened between the spacer adjacent to the bucking coil, and the iron flange. However, at the inner radius, about 6 kN of compressive contact is maintained. (see Table III). This compression is therefore available to resist the subsequent axial Lorentz forces of the bucking coil

The main coil spool continues to experience increased hoop loading. The corrected stresses in the central portion are 200 MPa.

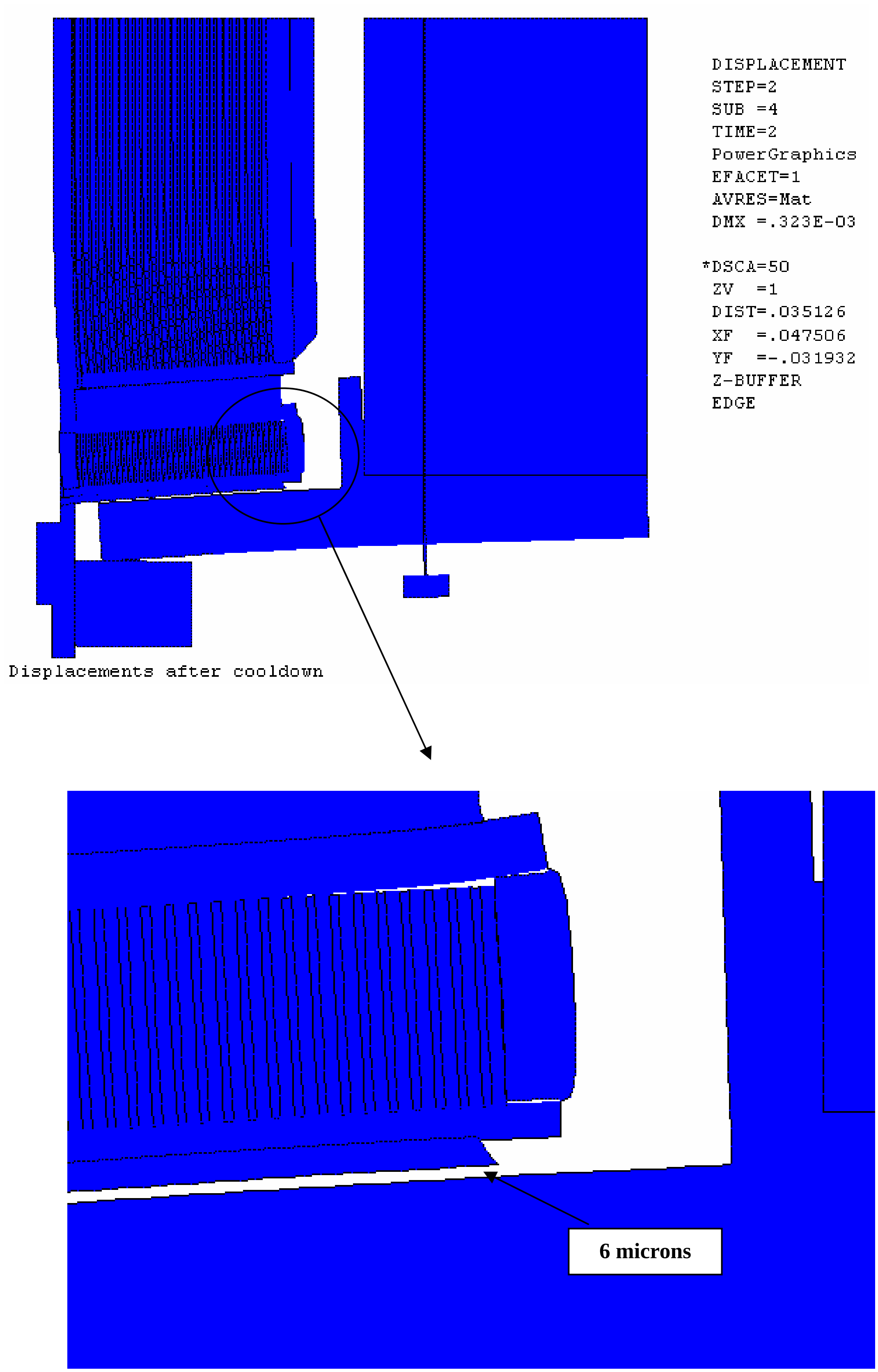


**Figure 4. Displacements after Cooldown**

## Energizing

The main coil and bucking coil currents of 188 amps was applied to generate the magnetic solution, and Lorentz forces for loading on the coils.

Fig. 5 shows the field solution. It is consistent with other calculation made on this geometry, producing a central field of 5.4 T, and very little stray field in the axial direction.

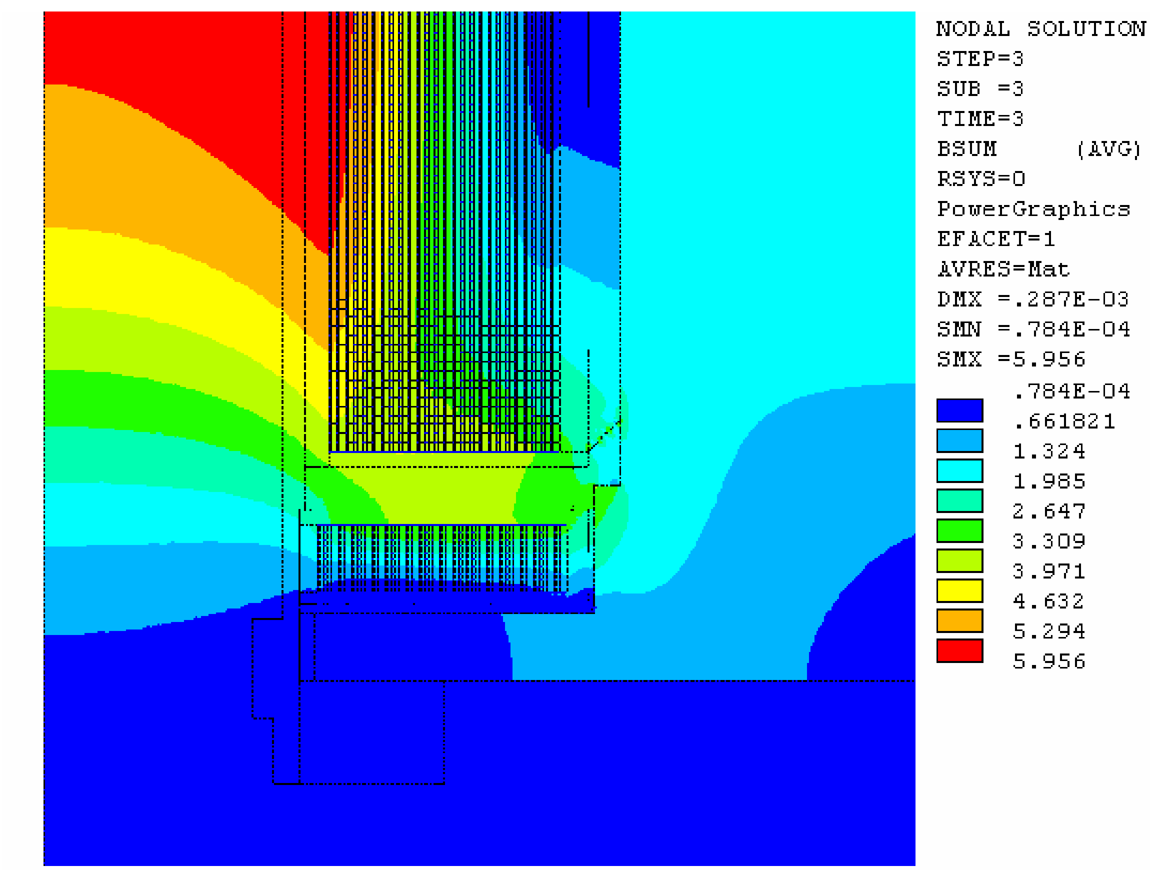


**Figure 5. Field Solution**

Fig. 6 shows the deflections after energizing. The bucking coils is in full contact with the iron flange, and the six micron gap is closed. Some axial contact still remains between the coils and spacers at the inner radius. The total force acting on the iron from the bucking coil is 18.1 kN.

The total axial Lorentz force acting on the bucking coil is 26.3 kN. Therefore, because of the preloading, about 8 kN of the Lorentz force was sustained by the release of compression in the preloaded coil assembly.

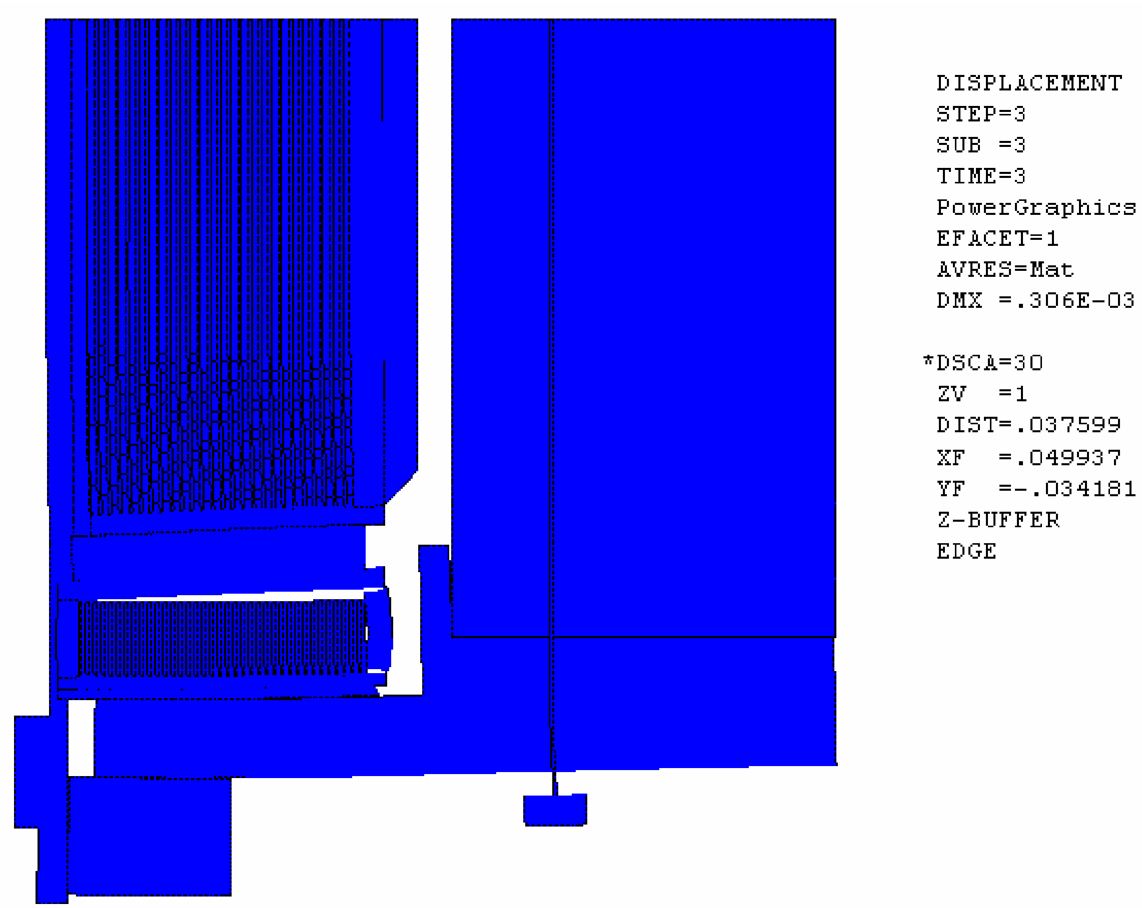


**Figure 6. Energizing**

The axial bucking coil deflections are shown in Fig. 7. The maximum deflection is about 24 microns, and occurs at the outer radius.

The main coil windings remain in contact with the spool and each other at all locations; in the bucking coil, a small amount of separation occurs in the region indicated in Fig. 8.

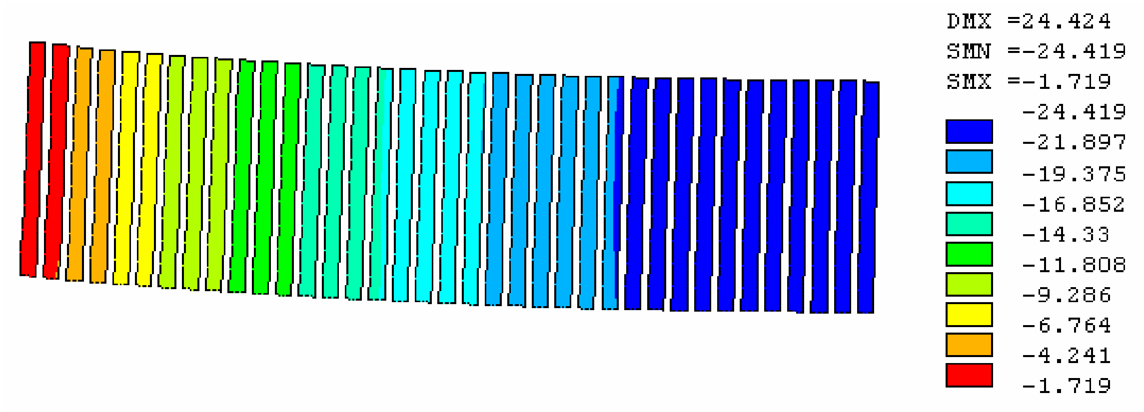


**Figure 7. Displacements of Bucking Coil (μm)**

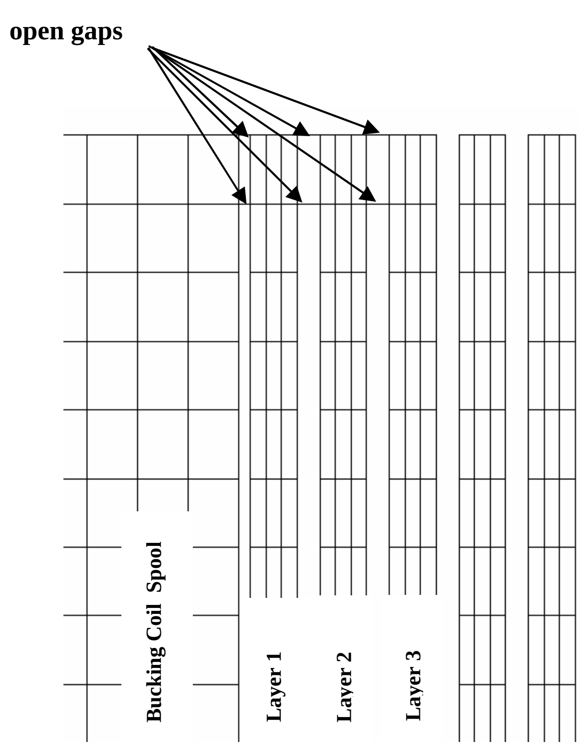


**Figure 8. Open Gaps in Bucking Coil after Energization**

## Forces on Iron

Table III shows the balance of forces on the iron and helium tube for the three load steps. The location and description of the forces is shown in Fig. 9. The values are consistent with a simple vector sum of forces in the axial direction, i.e., the sum of the helium tube force and the thru-bolt force must equal the force on the iron flange from the compressed coils.

The table shows that about 7 kN of the original 27 kN of compression is retained after cool down. This allows the decompression of the coils to increase the stiffness of the system, and reduce the axial displacements of the bucking coils.

**Table III. Force Balance on the Iron/He Tube System**

| Load Step | Force on Component (see Fig 9 ) kN | | |
|---|---|---|---|
| | Helium Tube | $F_{bolt}$ | $F_{coils}$ |
| Warm Preload/Assembly | 13.5 | 13.8 | -27.3 |
| Cool down | 1.8 | 5.1 | -6.9 |
| Energize | 5.7 | 12.4 | -18.1 |

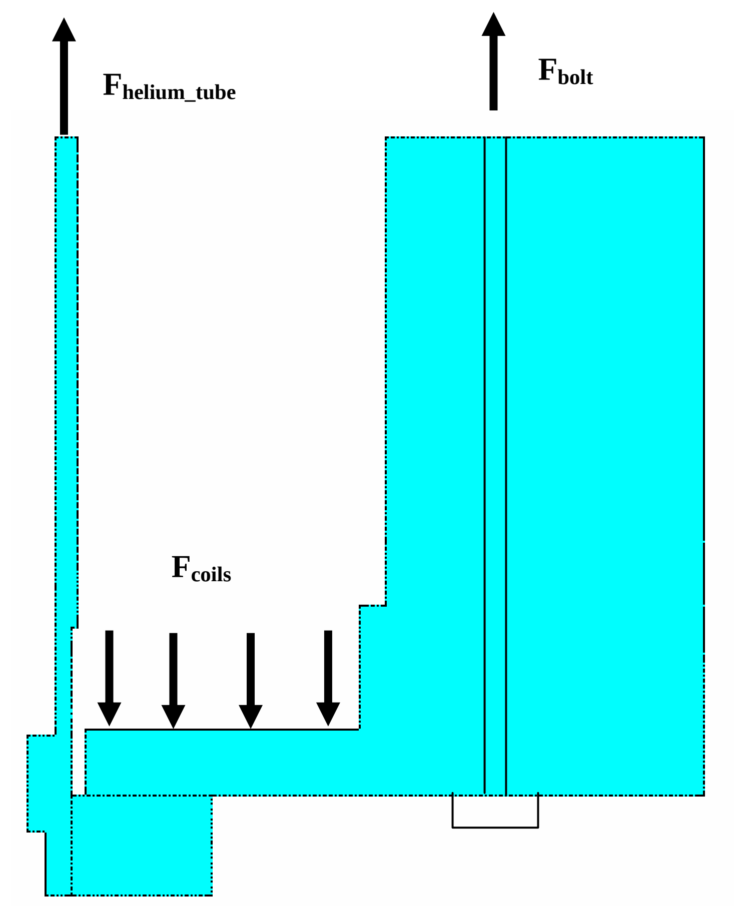


**Figure 9. Forces in Table III**

**Stresses in Iron**

The iron stresses were evaluated at the section A-B shown in Fig. 10. The ANSYS PRSE command was used to linearize the FEA solution, decomposing it into membrane and bending components.

The maximum membrane+bending stress intensity in the section is about 21 MPa (3 ksi). Carbon steel should have no difficulties sustaining this stress at liquid helium temperatures.

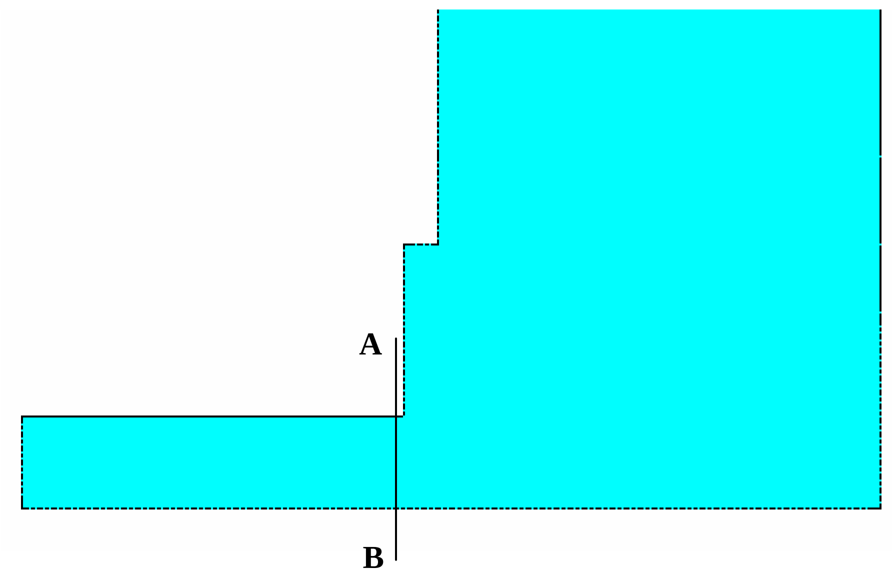


**Figure 10. Section Through Iron Flange for Stress Evaluation**

## Conclusions

The following observations may be made as a result of this analysis:

1. A winding tension of 20 N for the main coil, combined with the additional preloading produced by differential thermal contractions during cool down, prevents the separation of the main coil windings from each other or the spool during energization.
2. A winding tension of 10 N for the bucking coil is sufficient to keep all but a small region in contact under the same circumstances.
3. Some yielding of the solenoid spool may result from winding. However, this yielding will at worst cause the spool to make contact with the helium tube, from which it will gain additional stiffness.
4. The magnetic solution shows that the design produces the expected field.
5. The compressive preload produced during assembly by interaction of the He tube and iron thru-bolts with the coil assembly is sufficient to keep the coil assembly in a state of compression after cooldown.
6. A small axial gap of 6 microns may open up between the bucking coil and adjacent components during cooldown at the outer radius of the coil. However, compression is maintained at smaller radii, and overall axial bucking coil displacements are only 24 microns after energizing.
7. A substantial portion of the axial Lorentz forces is reacted by the relief of compressive preload in the coil assembly.
8. The stresses in the carbon steel are low, and should cause no concern.